



Dissemination patterns of Hodgkin lymphoma using a probability network model based on [¹⁸F]-FDG PET/CT

Mehdi Mouheb¹ · Morgane Pierre-Jean² · Christophe Fermé³ · Anne Devillers¹ · Thierry Lamy⁴ · Florence Le Jeune¹ · Roch Houot⁴ · Xavier Palard-Novello¹

Received: 10 November 2022 / Accepted: 9 December 2022 / Published online: 16 December 2022
© The Author(s), under exclusive licence to Springer-Verlag GmbH Germany, part of Springer Nature 2022

Abstract

Purpose The preferred hypothesis for the dissemination patterns of Hodgkin lymphoma (HL) is the contiguity hypothesis. However, this hypothesis is based on studies performed before the advent of [¹⁸F]-FDG PET/CT which is now the established reference for HL staging. This study aims to extract the dissemination patterns of HL using [¹⁸F]-FDG PET/CT and a probability network model.

Methods We retrospectively analyzed [¹⁸F]-FDG PET/CT performed for initial staging of patients with classical HL. The HL involvement status (presence of absence) was reported for 19 supra- and infra-diaphragmatic lymph node regions and 4 extranodal regions (lung, spleen, liver, and osteo- medullary). The analysis of HL dissemination was carried out using HL involvement status for all regions through 3 distinct methods: comparison of nearby lymph node regions, correlation assessment between all regions and relationship strength between all regions using Ising network model.

Results A total of 196 patients were included. Our results showed strong relationships between nearby involved lymph node regions (for example between the left pelvic and the abdominal lymph node regions (relationship strength = 0.980)) and between more distant regions (for example between right and left axillary lymph node regions (strength = 0.714)). Furthermore, involvement of the infra-diaphragmatic lymph node regions was significantly correlated with Ann Arbor stage IV ($\phi = 0.56$, $p < 0.001$).

Conclusion This study confirms the hypothesis of lymphatic dissemination of HL in a contiguous mode, with additional links between more distant regions. These predictable dissemination patterns could be useful for the initial staging assessment of patients with HL using [¹⁸F]-FDG PET/CT.

Keywords [¹⁸F]-FDG PET/CT · Hodgkin lymphoma · Dissemination · Network

Introduction

Predictable dissemination patterns could be useful for the initial staging assessment of patients with Hodgkin lymphoma (HL) using 2-fluoro-2-deoxy-D-glucose positron emission tomography/computed tomography ([¹⁸F]-FDG PET/CT). The preferred hypothesis for lymphatic dissemination is the so-called contiguity theory. The contiguity theory suggests that HL disease spreads from an initial involved lymph node region to other lymph node regions along lymphatic channels. Rosenberg and Kaplan first studied it in 1966 [1]. However, Smithers et al. suggested another hypothesis so-called “susceptibility theory” a few years later [2, 3]. Authors hypothesized that HL is spread by a causative agent with de novo induction in different sites, for example viral. The remaining lymph node regions

This article is part of the Topical Collection on Hematology.

✉ Xavier Palard-Novello
x.palard@rennes.unicancer.fr

¹ Univ Rennes, CLCC Eugène Marquis, INSERM, LTSI - UMR 1099 Rennes, France

² Univ Rennes, CHU de Rennes, INSERM, LTSI - UMR 1099 Rennes, France

³ CLCC Gustave Roussy, Villejuif, France

⁴ Univ Rennes, CHU de Rennes, INSERM, BIGRES - UMR 1236 Rennes, France

would have an independent probability of being the next ones involved. Lymphography was the imaging modality used on the previous studies. Until the 1990s, this imaging modality was considered as the best investigation for evaluating the deep lymph nodes of patients with lymphoma [4]. Then, spiral multi-slice computed tomography (CT) replaced lymphography due to better performances for detecting HL lesions [5]. Compared to lymphography, CT is less invasive and enables detection of nodal and extranodal lesions. However, [¹⁸F]-FDG PET/CT is now recognized as the reference standard for the initial staging of patients with HL because it demonstrated excellent performance to detect simultaneously HL nodal and extranodal lesions in the whole body [6]. [¹⁸F]-FDG PET/CT has the same advantages as CT compared to lymphography, and outperforms CT for staging newly diagnosed HL [7], especially for osteo-medullary involvement [8]. To the best of our knowledge, there is no study that already assessed dissemination patterns of HL using [¹⁸F]-FDG PET/CT. The study aims to analyze the distribution of involved nodal and extranodal regions using [¹⁸F]-FDG PET/CT in order to extract the dissemination patterns of HL using a probability network model.

Material and methods

Patients

Patients aged ≥ 18 years with classic HL who performed [¹⁸F]-FDG PET/CT between 2009 and 2021 at the Eugene Marquis Center (Rennes, France) for initial staging were retrospectively included. Age, gender, histological subtype of HL, B-symptoms status (presence or absence unexplained unintentional weight loss of 10% within 6 months or night sweats or unexplained fever $> 38^{\circ}\text{C}$), and Epstein-Barr virus (EBV) status (presence or absence of surrogate marker of EBV extracted from the pathological analysis) were collected. This study was approved by the local institutional review board of the University Hospital of Rennes (IRB-No. 21/94).

[¹⁸F]-FDG PET/CT data

[¹⁸F]-FDG PET/CT scans were acquired using 4 different PET/CT systems (Discovery ST (General Electric Healthcare), Biograph mCT (Siemens Healthineers), Biograph mCT flow (Siemens Healthineers) and Discovery MI (General Electric Healthcare)). The recommended interval between FDG administration and the start of acquisition was 60 minutes [9]. PET/CT scans were acquired at least from skull base to proximal thighs. PET/CT images were

analyzed by a nuclear medicine physician using Syngo via software (Siemens Healthineers). Every focal tracer uptake deviating from physiological distribution and background was regarded as suggestive of HL lesion. The HL involvement status (presence or absence) was reported for 19 supra- and infra-diaphragmatic lymph node regions and 4 extranodal regions (lung, spleen, liver, and osteo-medullary region). For each patient, the region with the maximal intensity of pathological uptake was reported (maximal Standardized Uptake Value (SUV_{max})). For each voxel, the SUV_{body weight} was obtained with the following formula:

$$\text{SUV body weight} = \frac{\text{activity concentration (Bq/mL)}}{\text{injected activity (Bq)/body weight (g)}}$$

Lymph node region status involvement and patient characteristics

Correlation assessment between involvement status of 4 lymph node regions (cervical, axillary, mediastinal/hilar, and infra-diaphragmatic), and age (> 35 or ≤ 35), gender, B-symptoms status, Ann Arbor stage IV status, and EBV status was performed using the phi correlation test which calculates the degree of association between two binary variables [10]. Absolute values of phi from 0 to 0.29 were regarded as weak correlation, from 0.30 to 0.59 as moderate correlation, and from 0.60 to 1.00 as strong correlation.

Assessment of HL dissemination

Regarding the HL dissemination assessment, a total of 185 patients were included because patients with Ann Arbor Stage I ($N = 11$) were excluded.

Comparison of the nearby lymph node regions involvement status

Pairs of adjacent lymph node regions were defined as follows (lymph node region 1/lymph node region 2): upper right cervical/lower right cervical, upper left cervical/lower left cervical, lower right cervical/right supra-clavicular, lower left cervical/left supra-clavicular, right supra-clavicular/right axillary, left supra-clavicular/left axillary, right supra-clavicular/upper mediastinum, left supra-clavicular/upper mediastinum, upper mediastinum/lower mediastinum, upper mediastinum/left hilar, upper mediastinum/right hilar, lower mediastinum/left hilar, lower mediastinum/right hilar, right internal mammary/right

costo-phrenic, left internal mammary/left costo-phrenic, abdominal/left pelvic, abdominal/right pelvic lymph node region. The frequency of simultaneous involvement of the pairs was compared with that expected with a χ^2 distribution.

Correlation analysis between the involvement status of the different regions

Correlation assessment between the involvement status of the different lymph node and extranodal regions was performed using the phi correlation test. Absolute values of phi from 0 to 0.29 were regarded as weak correlation, from 0.30 to 0.59 as moderate correlation, and from 0.60 to 1.00 as strong correlation.

Ising network model

The Ising model has been used to infer a graph structure that estimates the relations between the different lymph node and extranodal regions. The method combines logistic regression with model selection using a LASSO regularization to obtain a sparse network [11]. To select the optimal parameter of the LASSO regularization, we used the extended Bayesian information criterion (EBIC). The mathematical model is described in the Supplementary Information 1. The links between the different regions are illustrated with edges in the network. To measure the strength of edges, bootstrapping was performed (500 resamples of the original dataset). The strength value of each edge refers to the frequency of the edge selected in the 500 bootstraps. Values of strength from 0 to 0.29 were regarded

as weak strength, from 0.30 to 0.59 as moderate strength, and from 0.60 to 1.00 as strong strength.

Statistical analysis

$p < 0.05$ was considered statistically significant. The Bonferroni correction was applied for multiple comparisons. Statistical analysis was performed using R software version 3.6.0 [12].

Results

Patients

A total of 196 patients were included after exclusion of 9 with concomitant hematological disease (6 with post-transplant lymphoproliferative disorders and 3 with chronic lymphocytic leukemia), exclusion of 16 patients because [^{18}F]-FDG PET/CT were not analyzable (8 with corrupted data, 5 with brown fat activity, 2 with hyperinsulinism, and 1 with image artifact), and 1 patient was excluded for extranodal involvement only (Fig. 1).

The median age of the patients was 35 years (range 18–89). There was a balanced distribution regarding the gender (54% of men) and the B-symptoms (47% of patients had B-symptoms). There was 28% of the patients with Ann Arbor stage IV and only 5.5% with Ann Arbor stage I. The most common histological subtype was the nodular sclerosis subtype (79%). The patient characteristics are summarized in Table 1.

Fig. 1 Flowchart

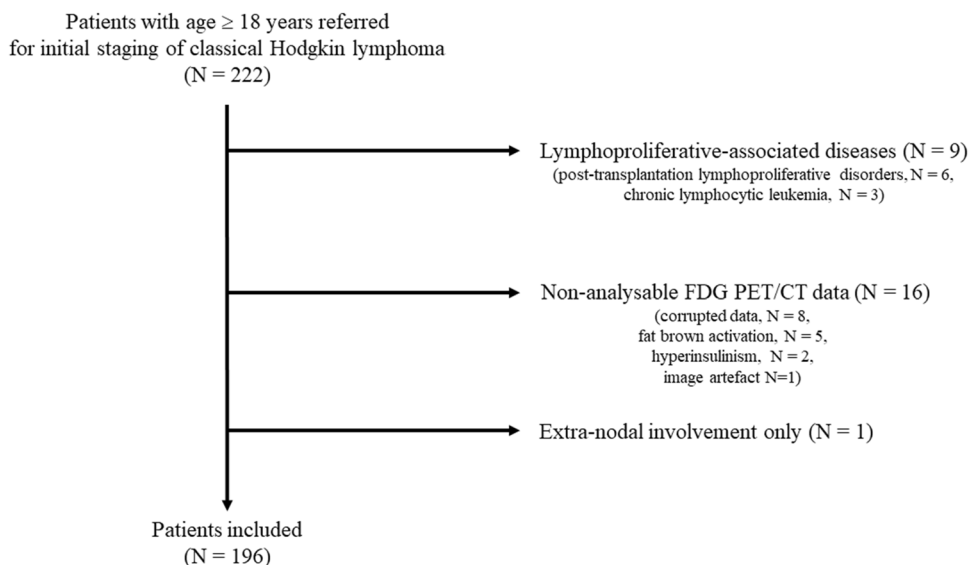


Table 1 Patient characteristics ($N=196$)

Characteristics	Value
Age (years), median (range)	35 (18–89)
Gender, n (%)	
Men	106 (54%)
Women	90 (46%)
Ann Arbor stage, n (%)	
I, supra-diaphragmatic/infra-diaphragmatic	11 (5.5%), 7/4
II, supra-diaphragmatic/infra-diaphragmatic	101 (51.5%), 97/4
III	29 (15%)
IV	55 (28%)
Subtype, n (%)	
Nodular sclerosis	156 (79.5%)
Mixed cellularity	10 (5%)
Lymphocyte-rich	4 (2%)
N/A	26 (13.5%)
B-symptoms, n (%)	
Presence	92 (47%)
Absence	104 (53%)
EBV status, n (%)	
Positive	96 (49%)
Negative	58 (30%)
N/A	42 (21%)

n , number of patients; N/A, non-available

Description of involved lymph node and extranodal regions

A sum of 1141 lymph node regions were involved in the 196 patients, with an average of 7 involved lymph node regions per patient (range 1–19). The most frequent involved region was the upper mediastinum lymph node region (164 patients, 84%). The right cardio-phrenic lymph node region was the least frequent involved lymph node region (35 patients, 18%) (Fig. 2). Splenic, osteo-medullary, hepatic, and pulmonary involvement were respectively found in 45 patients (23%), 42 patients (21%), 16 patients (8%), and 16 patients (8%). The SUVmax was most frequently measured in the upper mediastinum lymph node region (61 patients, 31%) and was never measured in the right or left cardio-phrenic lymph node regions.

Lymph node region status involvement and patient characteristics

The results showed a moderate correlation between infra-diaphragmatic lymph node region involvement and age > 35 years ($\phi = 0.39$, $p < 0.001$), male gender ($\phi = 0.33$, $p < 0.001$), B-symptoms ($\phi = 0.32$, $p < 0.001$), and Ann Arbor stage IV ($\phi = 0.56$, $p < 0.001$). Our results showed

also a significant but weak correlation between cervical lymph node involvement and age > 35 years ($\phi = 0.20$, $p < 0.029$) and between mediastinal/hilar involvement and female gender ($\phi = 0.29$, $p = 0.001$). No significant correlation was observed between lymph node regions involvement status and EBV status. The results are summarized in Table 2.

Assessment of HL dissemination

Comparison of the nearby lymph node regions involvement status

The number of simultaneous adjacent involved lymph node regions were 1121, whereas the number expected with a χ^2 distribution were 727 ($p < 0.001$) (Table 3). Nearby lymph node regions were more frequently involved than expected, suggesting contiguous dissemination.

Correlation analysis between the involvement status of the different regions

Our results showed a significant correlation of the involvement status between different nearby lymph node regions (for example between the left pelvic and the abdominal lymph node regions ($\phi = 0.63$), between the lower left cervical and the left supra-clavicular lymph node regions ($\phi = 0.50$), or between the right axillary and the right supra-clavicular lymph node regions ($\phi = 0.28$)).

The results showed also a significant but moderate correlation between several distant lymph node regions (for example between the right and left upper cervical lymph node regions ($\phi = 0.37$), between the right and left axillary lymph node regions ($\phi = 0.37$), and between the right and left internal mammary lymph node regions ($\phi = 0.61$)).

A strong correlation was found between the abdominal lymph node region and the spleen ($\phi = 0.60$). No significant correlation was found between the abdominal and the left supra-clavicular lymph node region. The correlation results between all regions are detailed in Supplementary Information 2.

Ising network model

Strong links were found between adjacent lymph node regions in the probabilistic Ising network model (for example between the lower left cervical and the left supra-clavicular lymph node regions (strength = 1.000), between the lower mediastinum and the left hilar lymph node regions (strength = 0.994), between the left pelvic and the abdominal lymph node regions (strength = 0.939), or between the

Fig. 2 Frequency (%) of involved lymph node and extranodal regions. For each region, the font size of the letters is proportional to the frequency

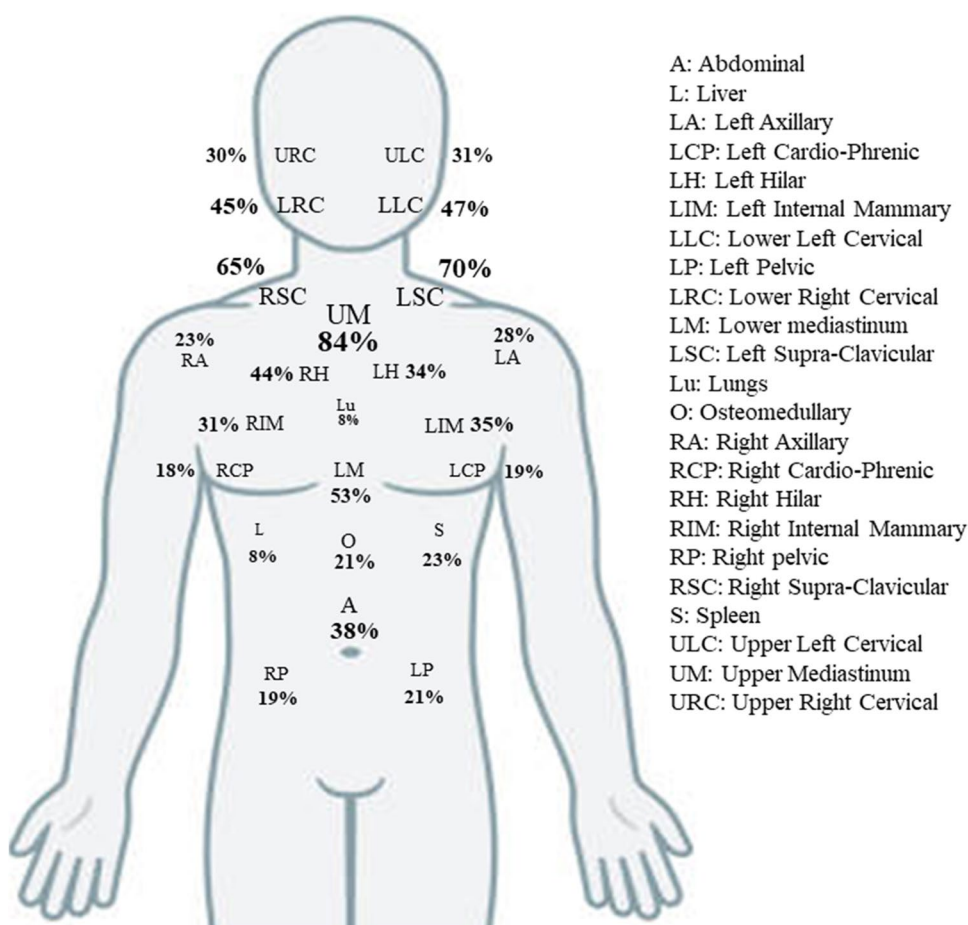


Table 2 Correlation assessment of lymph node regions involvement status and patient characteristics

Involved lymph node region	Age > 35	Female gender	B-symptoms	Ann Arbor stage IV	Surrogate marker of EBV
Cervical	-0.20/> 0.029*	-0.05/1.000	0.06/1.000	0.07/1.000	-0.02/1.000
Axillary	-0.01/1.000	-0.06/1.000	0.11/0.703	0.17/0.109	-0.04/1.000
Supra-clavicular	-0.17/0.118	0.14/0.322	0.12/0.522	0.09/1.000	-0.19/0.136
Mediastinal/hilar	-0.15/0.247	0.29/0.001*	0.10/0.880	0.15/0.246	-0.16/0.348
Infra-diaphragmatic	0.39/< 0.001*	-0.33/< 0.001*	0.32/< 0.001*	0.56/< 0.001*	0.08/1.000

Phi correlation value/*p*-value with Bonferroni correction, **p*-value < 0.05
EBV, Epstein-Barr virus

upper mediastinum and the right supra-clavicular lymph node regions (strength = 0.762)).

The model showed also strong links between several distant regions (for example between right and left pelvic lymph node regions (strength = 1.000), between right and left internal mammary lymph node regions (strength = 1.000), between right and left cardio-phrenic lymph node

regions (strength = 0.982), or between right and left axillary lymph node regions (strength = 0.713)).

A strong relationship was found between the abdominal lymph node region and the spleen (strength = 1.000). The relationship strength results between all regions are detailed in the Supplementary Information 3. Strong links (strength > 0.6) between regions are displayed in Fig. 3.

to explore associations between sites of involvement. Associations between adjacent lymph node regions were found, so authors concluded that HL spreads contiguously. Then, Roth et al. analyzed lymphatic dissemination as a function of distribution involvement using also lymphography with also physical examination, lymphography, and histopathologic findings including 297 patients [14]. Authors compared the number of gaps observed for the different pattern of distribution with the number expected according to a probability model for random progression. Authors concluded also that HL spreads via functionally contiguous lymph nodes.

In relation to the significant link between distant lymph node regions, Mauch et al. already exhibited an association between right and left cervical lymph node regions and right and left axillary lymph node regions [13]. The creation of a collateral lymphatic network linked to the obstruction of the main lymphatic network by the invasion and thus the enlargement of the lymph nodes could be an explanation for the association between these distant lymph node regions. This explanation is supported by the results of an experimental study suggested that the ligation of the thoracic duct led to the opening of pre-existing collateral lymphatic networks [15]. Moreover, using lymphography, lymphatic obstruction may be revealed in patients with the lymph flows via collaterals within regions not usually permeated [16].

Concerning the significant correlation between infra-diaphragmatic involvement and age > 35 years, male gender, B-symptoms, and Ann Arbor stage IV, Mauch et al. already showed an association between infra-diaphragmatic involvement and age > 35 years and the presence of B-symptoms [11]. Related to these findings, different studies exhibited an association between isolated infra-diaphragmatic HL and older age [17–20] and male gender [17–21]. No hypothesis in literature has been suggested to explain these correlations. Furthermore, the results of our study show a significant correlation between infra-diaphragmatic involvement and extranodal involvement. However, only 8 patients (4%) have involvement limited to the infra-diaphragmatic lymph node regions, which is consistent with literature (only 3–11% of adult patients have an isolated infra-diaphragmatic HL [18]). The risk of hematogenous dissemination of HL is probably higher with HL disseminated on both sides of the diaphragm than involvement limited to one side, which could be an explanation for the association between infra-diaphragmatic involvement and extranodal involvement. This could also explain the correlation of infra-diaphragmatic involvement in our study with the presence of B-symptoms. Indeed, the presence

of B-symptoms is more frequent in patients with an advanced stage [21].

Whether through correlation analysis or the Ising network model, no significant association was observed between the abdominal lymph node region and the left supra-clavicular lymph node region. However, the presence of a lymphatic pathway linking the chyle cistern (or Pecquet's cistern) and the left jugulo-subclavian venous confluence via the thoracic duct is known from anatomical description [22]. On one hand, different studies confirmed the existence of a link between the abdominal lymph node region and the left supra-clavicular lymph node region [2, 23, 24]. On the other hand, a lymphatic dissemination from the abdominal lymph node region to the mediastinal/hilar lymph node regions was exhibited in two studies [13, 14]. However, the results of our study did not reveal any association between these regions neither. As suggested by Mann et al., the link between the supra-diaphragmatic lymph node regions and the abdominal lymph node regions could be the spleen [25]. Indeed, the authors suggested an hematogenous dissemination to the spleen and a lymphatic dissemination from the spleen to the abdominal lymph node regions. In anatomical description, the spleen has only efferent lymphatic vessels [26], which is consistent with this hypothesis. In our study, results showed a strong relationship between the spleen and the abdominal lymph node region. Moreover, our results exhibited a strong link between spleen involvement and liver involvement, suggesting an hematogenous dissemination to the spleen. So, if we consider in our study that most of the patients with infra-diaphragmatic involvement have a supra-diaphragmatic origin of HL, most of the involved abdominal lymph node regions could come from the spleen. However, the results of our study do not exhibit a strong link between the lymphovenous junctions (supra-clavicular lymph node regions) and the spleen.

This study has some limitations. Firstly, it is a retrospective study, which may lead to possible selection bias. Secondly, HL involvement in the different regions has been assessed by [¹⁸F]-FDG PET/CT, with a risk of false positive or false negative. Thirdly, [¹⁸F]-FDG PET/CT scans were performed on different systems with different detection efficiency. For instance, involved lymph node regions with low [¹⁸F]-FDG uptake could be missed using a PET/CT device with a low detection efficiency whereas it could be detected using a high-performance PET/CT device. However, no quantitative metrics were compared in this study. Fourthly, the impossibility to define the initially involved lymph node region did not allow to model an oriented probabilistic network model.

To the best of our knowledge, we report the first lymphoma dissemination patterns obtained from a probabilistic network model which enables to assess the relationship strength between all regions simultaneously.

Conclusion

This study confirms the hypothesis of lymphatic dissemination of HL in a contiguous mode and exhibits additional link between more distant lymph node regions. This predictable pattern of spread could be useful for the initial staging assessment of patients with HL using [¹⁸F]-FDG PET/CT.

Supplementary Information The online version contains supplementary material available at <https://doi.org/10.1007/s00259-022-06086-z>.

Author contribution RH and XPN contributed to the study conception and design. Data collection were performed by MM and XPN. MPJ performed statistical analysis. The first draft of the manuscript was written by MM. All authors were involved in review of the manuscript and approved the final manuscript.

Data availability The datasets generated during and/or analyzed during the current study are available from the corresponding author on reasonable request.

Declarations

Ethics approval This study was approved by the local institutional review board of the University Hospital of Rennes (IRB-No. 21/94) and performed in accordance with the Declaration of Helsinki. Written, informed consent was waived for this retrospective analysis.

Competing interests The authors declare no competing interests.

References

- Rosenberg SA, Kaplan HS. Evidence for an orderly progression in the spread of Hodgkin's disease. *Cancer Res.* 1966;26(6):1225–31.
- Smithers DW, Lillcrap SC, Barnes A. Patterns of lymph node involvement in relation to hypotheses about the modes of spread of Hodgkin's disease. *Cancer.* 1974;34(5):1779–86. [https://doi.org/10.1002/1097-0142\(197411\)34:5%3c1779::aid-cnrc2820340528%3e3.0.co;2-5](https://doi.org/10.1002/1097-0142(197411)34:5%3c1779::aid-cnrc2820340528%3e3.0.co;2-5).
- Smithers DW. Spread of Hodgkin's disease. *Lancet.* 1970;1(7659):1262–7. [https://doi.org/10.1016/s0140-6736\(70\)91743-5](https://doi.org/10.1016/s0140-6736(70)91743-5).
- Guermazi A. Is it wise to eliminate lymphography from the staging of Hodgkin's disease? *Leuk Lymphoma.* 2001;42(4):655–60. <https://doi.org/10.3109/10428190109099326>.
- Sombeck MD, Mendenhall NP, Kaude JV, Torres GM, Million RR. Correlation of lymphangiography, computed tomography, and laparotomy in the staging of Hodgkin's disease. *Int J Radiat Oncol Biol Phys.* 1993;25(3):425–9. [https://doi.org/10.1016/0360-3016\(93\)90063-2](https://doi.org/10.1016/0360-3016(93)90063-2).
- Salaün PY, Abgral R, Malard O, Querellou-Lefranc S, Quere G, Wartski M, et al. Actualisation des recommandations de bonne pratique clinique pour l'utilisation de la TEP en cancérologie [Update of the recommendations of good clinical practice for the use of PET in oncology]. *Bull Cancer.* 2019;106(3):262–74. <https://doi.org/10.1016/j.bulcan.2019.01.002>.
- Kwee TC, Kwee RM, Nievelstein RA. Imaging in staging of malignant lymphoma: a systematic review. *Blood.* 2008;111(2):504–16. <https://doi.org/10.1182/blood-2007-07-101899>.
- Adams HJ, Kwee TC, de Keizer B, Fijnheer R, de Klerk JM, Littooi AS, et al. Systematic review and meta-analysis on the diagnostic performance of FDG-PET/CT in detecting bone marrow involvement in newly diagnosed Hodgkin lymphoma: is bone marrow biopsy still necessary? *Ann Oncol.* 2014;25(5):921–7. <https://doi.org/10.1093/annonc/mdt533>.
- Boellaard R, O'Doherty MJ, Weber WA, Mottaghy FM, Lonsdale MN, Stroobants SG, et al. FDG PET and PET/CT: EANM procedure guidelines for tumour PET imaging: version 1.0. *Eur J Nucl Med Mol Imaging.* 2010 Jan;37(1):181–200. <https://doi.org/10.1007/s00259-009-1297-4>.
- McHugh ML. "Phi Correlation Coefficient." *The SAGE Encyclopedia of Educational Research, Measurement, and Evaluation.* Edited by Bruce B. Frey. Thousand Oaks.: SAGE Publications, Inc., 2018, pp. 1252–1253. <https://doi.org/10.4135/9781506326139>.
- van Borkulo CD, Borsboom D, Epskamp S, Blanken TF, Boschloo L, Schoevers RA, Waldorp LJ. A new method for constructing networks from binary data. *Sci Rep.* 2014;4(4):5918. <https://doi.org/10.1038/srep05918>.
- R Core Team (2019). R: A language and environment for statistical computing. R Foundation for Statistical Computing, Vienna, Austria. <https://www.R-project.org>
- Mauch PM, Kalish LA, Kadin M, Coleman CN, Osteen R, Hellman S. Patterns of presentation of Hodgkin disease. Implications for etiology and pathogenesis *Cancer.* 1993;71(6):2062–71. [https://doi.org/10.1002/1097-0142\(19930315\)71:6%3c2062::aid-cnrc2820710622%3e3.0.co;2-0](https://doi.org/10.1002/1097-0142(19930315)71:6%3c2062::aid-cnrc2820710622%3e3.0.co;2-0).
- Roth SL, Sack H, Havemann K, Willers R, Kocsis B, Schumacher V. Contiguous pattern spreading in patients with Hodgkin's disease. *Radiother Oncol.* 1998;47(1):7–16. [https://doi.org/10.1016/s0167-8140\(97\)00208-9](https://doi.org/10.1016/s0167-8140(97)00208-9).
- Blalock, Alfred et al. "Experimental studies on lymphatic blockage." *Archives of Surgery* 34 (1937): 1049–1071. <https://doi.org/10.1001/ARCHSURG.1937.01190120075005>
- Kinmonth JB, Taylor GW, Harper RK. Lymphangiography; a technique for its clinical use in the lower limb. *Br Med J.* 1955;1(4919):940–2. <https://doi.org/10.1136/bmj.1.4919.940>.
- Darabi K, Sieber M, Chaitowitz M, Braitman LE, Tester W, Diehl V. Infradiaphragmatic versus supradiaphragmatic Hodgkin lymphoma: a retrospective review of 1,114 patients. *Leuk Lymphoma.* 2005;46(12):1715–20. <https://doi.org/10.1080/10428190500144847>.
- Rossi C, Mounier M, Brice P, Safar V, Nicolas-Virelizier E, Rey P, Stamatoullas-Bastard A, Alcantara M, Chauchet A, Reboursière E, Filliatre L, Perrot A, Garcia S, Salles G, Coiffier B, Ghesquière H, Casasnovas RO. Infradiaphragmatic Hodgkin lymphoma: a large series of patients staged with PET-CT. *Oncotarget.* 2017 Jul 19;8(49):85110–85119. <https://doi.org/10.18632/oncotarget.19389>
- Sasse S, Goergen H, Plütschow A, Böll B, Eichenauer DA, Fuchs M, et al. Outcome of patients with early-stage infradiaphragmatic hodgkin lymphoma: a comprehensive analysis from the German Hodgkin study group. *J Clin Oncol.* 2018;36(25):2603–11. <https://doi.org/10.1200/JCO.2018.78.7192>.
- Vassilakopoulos TP, Angelopoulou MK, Siakantaris MP, Konstantinou N, Symeonidis A, Karmiris T, et al. Pure infradiaphragmatic Hodgkin's lymphoma. Clinical features, prognostic factor and comparison with supradiaphragmatic disease. *Haematologica.* 2006 Jan;91(1):32–9

21. Shanbhag S, Ambinder RF. Hodgkin lymphoma: a review and update on recent progress. *CA Cancer J Clin*. 2018;68(2):116–32. <https://doi.org/10.3322/caac.21438>.
22. Karamanou M, Laios K, Tsoucalas G, Machairas N, Androustos G. Charles-Emile Troisier (1844–1919) and the clinical description of signal node. *J BUON*. 2014 Oct-Dec;19(4):1133–5.
23. Lee BJ, Nelson JH, Schwarz G. Evaluation of lymphangiography, inferior venacavography and intravenous pyelography in the clinical staging and management of Hodgkin's disease and lymphosarcoma. *N Engl J Med*. 1964;13(271):327–37. <https://doi.org/10.1056/NEJM196408132710701>.
24. Negus D, Edwards JM, Kinmonth JB. Filling of cervical and mediastinal nodes from the thoracic duct and the physiology of Virchow's node—studies by lymphography. *Br J Surg*. 1970;57(4):267–71. <https://doi.org/10.1002/bjs.1800570407>.
25. Mann JL, Hafez GR, Longo WL. Role of the spleen in the trans-diaphragmatic spread of Hodgkin's disease. *Am J Med*. 1986 Dec;81(6):959–61. [https://doi.org/10.1016/0002-9343\(86\)90387-6](https://doi.org/10.1016/0002-9343(86)90387-6)
26. Weiss L. *Histology: cell and tissue biology*. New York: Elsevier Biomedical; 1983.

Publisher's note Springer Nature remains neutral with regard to jurisdictional claims in published maps and institutional affiliations.

Springer Nature or its licensor (e.g. a society or other partner) holds exclusive rights to this article under a publishing agreement with the author(s) or other rightsholder(s); author self-archiving of the accepted manuscript version of this article is solely governed by the terms of such publishing agreement and applicable law.